第 57 卷 第 3 期
2025 年 5 月

工　程　科　学　与　技　术
ADVANCED ENGINEERING SCIENCES

Vol. 57 No. 3
May 2025

•土木工程•

DOI:10.12454/j.jsuese.202400017

本刊网刊

考虑土体参数空间变异性的地震作用下无限长边坡可靠度研究

朱德胜[1]，夏　磊[2]，柯力俊[1]，王　震[1*]

(1.扬州大学 建筑科学与工程学院，江苏 扬州 225127；2.东南大学 土木工程学院，江苏 南京 211189)

摘　要：土体参数的空间变异性对地震边坡安全评价的影响不可忽视，采用概率分析的方法对地震边坡稳定性进行系统性研究十分必要。基于随机场方法分析水平和竖向地震力共同作用对无限长边坡可靠度的影响，并采用确定性分析方法相互验证。对比分析发现，在水平和竖向地震力共同作用下，即使水平地震力系数较小，竖向地震力对无限长边坡的失效概率仍有明显影响。同时，随着水平地震力系数增大，竖向地震力作用对最危险坡度的影响也逐渐增强。结果表明，对地震力作用下的无限长边坡进行可靠度分析时，水平和竖向地震力作用均不可忽略。

关键词：无限长边坡；地震力；最危险坡度；可靠度分析；随机场模拟

中图分类号：TU43　　**文献标志码：**A　　**文章编号：**2096-3246（2025）03-0106-09

全世界每年都有报道边坡失稳的问题，特别是地震引起的滑坡，严重威胁人民生命财产安全[1]。众多专家学者采用不同的方法对地震作用下的边坡稳定性进行了研究，包括拟静力法[2–5]、永久位移法[6–9]、有限元法[10–13]。然而，土体参数具有不确定性[14–16]，对边坡的稳定评价有重要影响。因此，采用概率分析方法对地震边坡稳定性进行研究十分必要。

边坡稳定分析方法中，基于无限长边坡方程的方法相对简单，可得到边坡安全系数的解析解[17]。现实中许多位于基岩上的山地边坡，其坡面长度远大于高度，即长边坡。该类边坡滑动面常与基岩表面平行，可视为无限长边坡破坏，在边坡稳定分析领域常用无限长边坡模型研究这一类浅层滑坡问题[18]。Griffiths等[19]提出随机场方法研究无限长边坡可靠度，土体强度参数由随机场理论生成，在模拟土体强度参数空间变异性时假定参数均值和方差不随深度的变化而改变。然而，土体不排水强度均值具有随深度增长的发展趋势[14]。Cai[20]和Zhu[21]等相继提出土体参数非平稳随机场模拟方法，研究无限长边坡可靠度。基于Zhu等[22]提出的不排水强度2维随机场模拟方法，Zhu等[23]对适用于无限长边坡土体的1维非平稳随机场进行模拟，分析了静力和水平地震力作用下土体不排水强度均值随深度线性增长的无限长边坡可靠度。然而，地震作用下的无限长边坡会同时受到水平和竖向地震影响，竖向地震力系数k_{v}的绝对值通常为水平地震力系数k_{h}的0.5~0.7倍，在震中及强震地区该比值可达到1.0以上[24]。本文对Zhu等[23]的工作进行拓展，研究水平和竖向地震力作用下无限长不排水和摩擦–黏性土边坡可靠度。研究成果将丰富边坡稳定可靠度分析理论。

1　无限长不排水边坡

1.1　确定性分析

以地震作用下土体不排水强度随深度线性增长的无限长边坡为例，其模型如图1所示。图1中，深色部分为无限长边坡单位宽度竖向土柱，β为边坡坡度，F为单位宽度竖向土柱两侧的侧向力，H为基岩上覆土体边坡高度，z为坡面至潜在破坏面的深度，c_{u0}为无限长边坡顶部土体不排水强度，c_{uz}为坡面以下深度z处土体不排水强度，ρ为土体不排水强度增长率。本文基于拟静力法，将地震力表示为地震力系数与无限长边坡单位宽度竖向土柱重量W的乘积，即水平地震力

收稿日期：2024 – 01 – 04　　**修回日期：**2024 – 03 – 27　　**网络出版日期：**2024 – 04 – 08

基金项目：国家自然科学基金项目（51808484；52308378）

作者简介：朱德胜（1987—），男，副教授．研究方向：岩土工程可靠度．E-mail：deshengzhu@yzu.edu.cn

* **通信作者：**王　震，讲师，E-mail：008094@yzu.edu.cn

为$k_{\mathrm{h}}W$、竖向地震力为$k_{\mathrm{v}}W$。为简化分析，不考虑地震引起的孔隙水压力，正的竖向地震力方向为竖直向下。

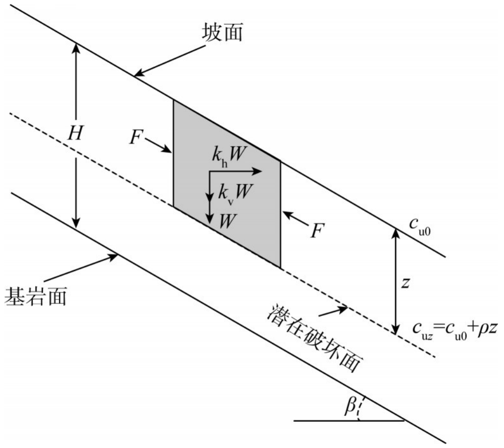

图1　地震作用下不排水强度随深度线性增长的无限长边坡模型

Fig. 1　A model for the infinite undrained slope with linearly increasing strength under seismic loadings

无限长边坡模型通常假定边坡坡面长度远大于边坡高度H，任取一单位宽度竖向土柱进行受力分析时，作用于竖向土柱两侧的侧向力F大小相等且方向相反。因此，边坡单位宽度竖向土柱两侧的侧向力相互抵消，只需考虑单位宽度竖向土柱潜在破坏面上的极限平衡。无限长边坡安全系数F_{S}为作用于单位宽度竖向土柱潜在破坏面上抗滑力与滑动力的比值[25]。则地震作用下土体不排水强度随深度线性增长的无限长边坡安全系数可表示为：

$$F_{\mathrm{S}}=\min\left(\frac{c_{\mathrm{u0}}+\rho z}{\left((1+k_{\mathrm{v}})\sin\beta+k_{\mathrm{h}}\cos\beta\right)\gamma z\cos\beta}\right) \tag{1}$$

式中，$0<z\leq H$，γ为土体重度。

由式(1)可知，当参数c_{u0}、ρ、γ、β、k_{h}、k_{v}保持不变时，最小值出现在无限长边坡最底部。因此，对于水平和竖向地震力作用下土体不排水强度随深度线性增长的无限长边坡，其安全系数为：

$$F_{\mathrm{S}}=\frac{c_{\mathrm{u0}}+\rho H}{\left((1+k_{\mathrm{v}})\sin\beta\cos\beta+k_{\mathrm{h}}\cos^2\beta\right)\gamma H} \tag{2}$$

$$f\left(\beta,k_{\mathrm{h}},k_{\mathrm{v}}\right)=(1+k_{\mathrm{v}})\sin\beta\cos\beta+k_{\mathrm{h}}\cos^2\beta \tag{3}$$

求解式(3)的最大值可获得最危险坡度$\beta_{\min}$(该坡度对应于F_{S}最小值)的解析解。对式(3)求导，得$\beta_{\min}$的解析解为：

$$\beta_{\min}=\frac{1}{2}\arctan\frac{1+k_{\mathrm{v}}}{k_{\mathrm{h}}} \tag{4}$$

为进一步研究地震作用下无限长不排水边坡的最危险坡度，算例边坡取值如下：$H=2.5$ m，$\gamma=20$ kN/m^3，$c_{\mathrm{u0}}=25$ kPa，$\rho=0.2$ kN/m^3。本文定义λ为竖向地震力系数与水平地震力系数比，即$\lambda=k_{\mathrm{v}}/k_{\mathrm{h}}$，$\lambda$取$-1.0$、$-0.5$、0、0.5、1.0。

图2为不同水平地震力系数下算例边坡的安全系数解析解(由式(2)计算)。由图2可知，当k_{h}一定时，随着λ的增大，F_{S}逐渐减小。这是因为当λ取负值时，竖向地震力$k_{\mathrm{v}}W$作用方向竖直向上，相当于减小了无限长边坡竖向土柱的自重，使边坡安全系数增大，通过式(2)也可验证该结论；同时，可观察到在水平和竖向地震力共同作用下，随着边坡坡度β增大，无限长边坡的安全系数F_{S}先减小后增大，这表明存在一个最危险坡度$\beta_{\min}$使边坡安全系数F_{S}取最小值。

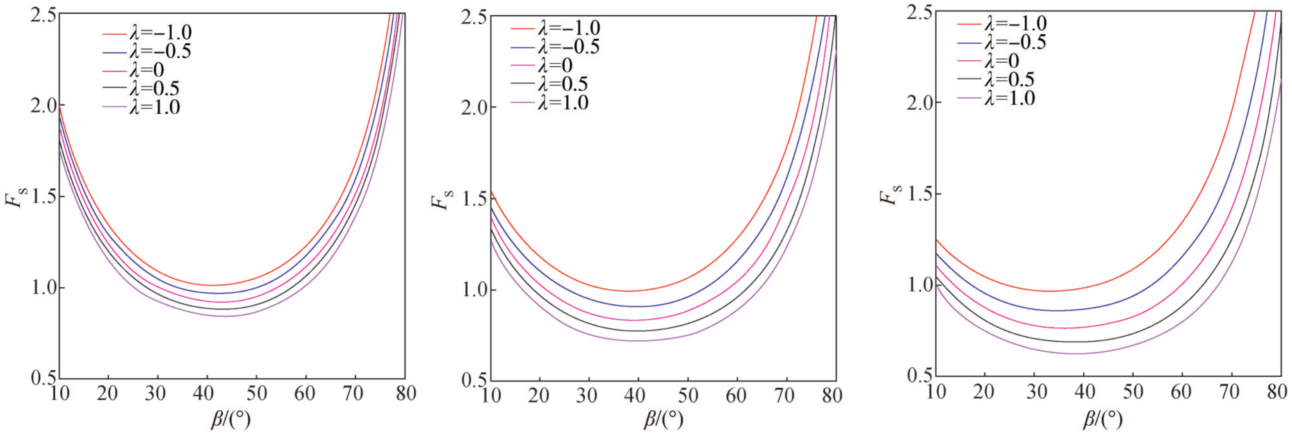

(a) k_{h}=0.1　(b) k_{h}=0.2　(c) k_{h}=0.3

图2　不同水平地震力系数下无限长不排水边坡安全系数

Fig. 2　Factors of safety for infinite undrained slope with different horizontal seismic coefficients

图3为不同水平地震力系数下，λ对无限长不排水边坡$\beta_{\min}$的影响。由图3可知，当k_{h}一定时，随着λ的增大，$\beta_{\min}$逐渐增大。随着λ从-1.0增大至1.0，当k_{h}=0.1时，$\beta_{\min}$增大约0.6°；当k_{h}=0.2时，$\beta_{\min}$增大约

2.3°；当k_h=0.3时，β_{min}增大约5.0°。说明随着k_h的增大，竖向地震力作用对无限长不排水边坡β_{min}的影响逐渐显著。β_{min}对初步评价无限长边坡地震稳定性有一定的参考作用。

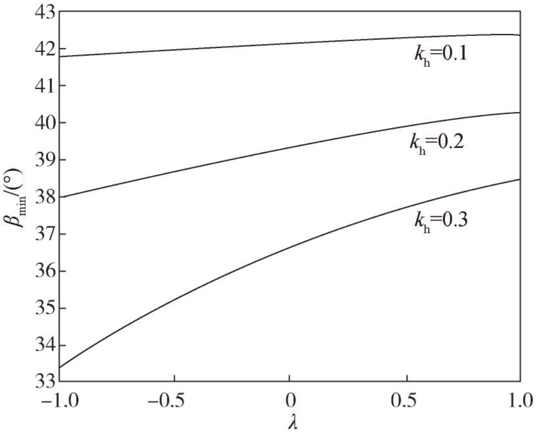

图3　不同水平地震力系数下无限长不排水边坡最危险坡度

Fig. 3　Critical slope angles for infinite undrained slopes with different horizontal seismic coefficients

1.2　可靠度分析

以土体不排水强度均值μ_{cuz}随深度线性增长的无限长边坡为例，μ_{cuz}随深度z变化可表示为：

$$\mu_{cuz}=\mu_{cu0}+\rho z \tag{5}$$

式中，μ_{cu0}为无限长边坡顶部土体不排水强度均值。

本文采用Zhu等[23]提出的无限长边坡土体不排水强度1维非平稳随机场模拟方法，其步骤如下：

1)采用局部平均法[26]，基于无限长边坡顶部(z=0)土体不排水强度参数统计信息，即均值σ_{cu0}、标准差σ_{cu0}和相关距离θ，生成初始的1维平稳的对数正态分布随机场，将该阶段生成的初始值c_{0i}赋值给无限长边坡所有单元。

2)考虑无限长不排水边坡其他深度(z>0)，将所有单元的土体不排水强度参数值采用比例因子进行调整，有：

$$c_{zi}=c_{0i}\frac{\mu_{cu0}+\rho z}{\mu_{cu0}} \tag{6}$$

式中，c_{zi}为第i个单元土体不排水强度参数值。

本文将无限长不排水边坡单位宽度竖向土柱划分为100个等厚单元，并将1维非平稳随机场方法生成的参数赋予各个单元。在每次蒙特卡罗模拟时，程序将计算每一个单元的安全系数(共100个)，其中，最小的安全系数即为无限长不排水边坡的安全系数。文献[19]表明，通过5 000次蒙特卡罗模拟可得到稳定的无限长边坡失效概率结果，本文同样取蒙特卡罗模拟次数为5 000，由5 000次蒙特卡罗模拟得到5 000个边坡安全系数值，无限长不排水边坡失效概率即为安全系数小于1的次数与5 000的比值。图4为计算无限长不排水边坡失效概率流程。

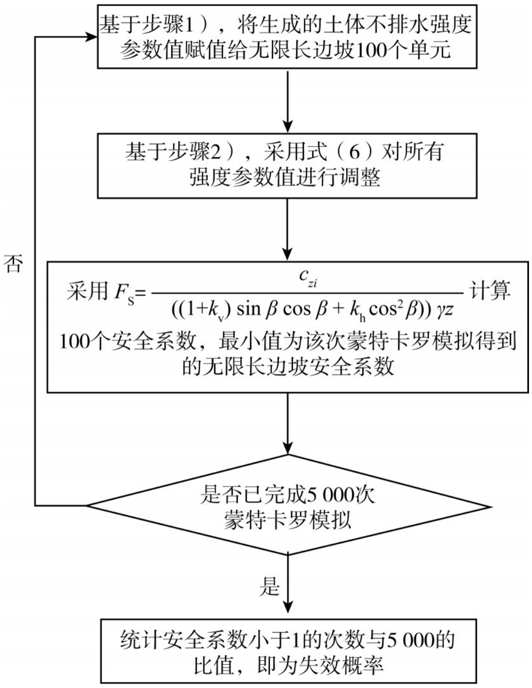

图4　计算无限长不排水边坡失效概率流程

Fig. 4　Flowchart for calculating probability of failure of infinite undrained slopes

为研究地震力对无限长不排水边坡可靠度的影响，算例边坡取值如下：μ_{cu0}=25 kPa，H=2.5 m，γ=20 kN/m^3，β=30°，不排水强度变异系数v_{cu}=0.1，ρ=0.2 kN/m^3，k_h=0.1；λ分别为－1.0、－0.5、0、0.5、1.0。本文采用1次2阶矩方法(FOSM)与随机场方法的计算结果进行对比。

图5为不同λ条件下无限长不排水边坡失效概率p_f与无量纲相关距离($\Theta=\theta/H$)的关系。由图5可知：在相同的Θ下，当λ从－1.0增大至1.0时，边坡失效概率显著增大，说明竖向地震力对无限长边坡可靠度的影响不可忽略；对于不同的λ，无限长边坡失效概率p_f随着无量纲相关距离Θ的增大而减小，最终收敛于FOSM计算结果，说明对地震作用下无限长不排水边坡采用传统的可靠度分析方法，会得到不保守的结果。

图6为地震力作用下无限长不排水边坡失效概率与边坡坡度的关系曲线。无限长边坡基本参数为：μ_{cu0}=25 kPa，H=2.5 m，γ=20 kN/m^3，ρ=0.2 kN/m^3，v_{cu}=0.1，Θ=4。由图6可知，当k_h=0.1、k_v=－0.05、β=42°时，边坡失效概率最大，由式(4)计算得到的β_{min}大约为42°。

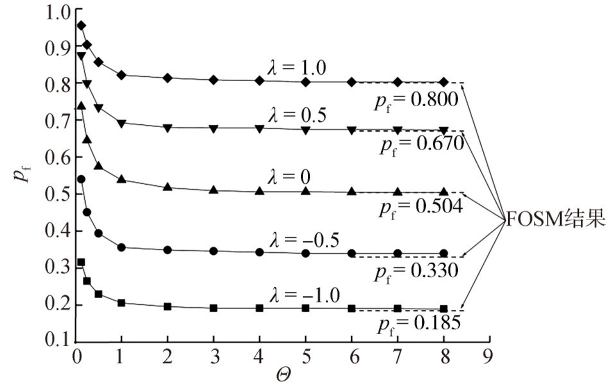

图5　不同λ条件下失效概率与无量纲相关距离关系曲线

Fig. 5　Probability of failure versus nondimensional spatial correlation length for different λ

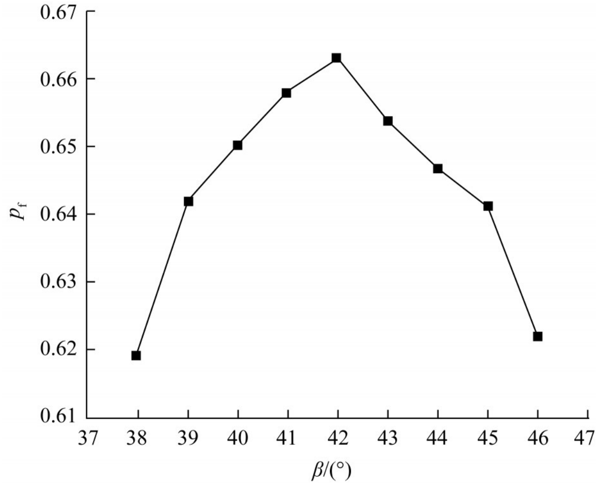

图6　边坡失效概率与边坡坡度关系曲线

Fig. 6　Probability of slope failure versus slope angle

2　无限长摩擦–黏性土边坡

2.1　确定性分析

图7为地震作用下无限长摩擦–黏性土边坡模型示意图。图7中,ϕ'为有效内摩擦角。

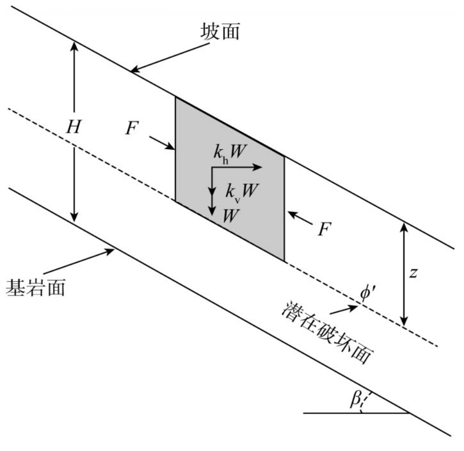

图7　地震作用下无限长摩擦–黏性土边坡模型示意图

Fig. 7　A model for an infinite cohesive–frictional soil slope under seismic loadings

地震作用下无限长摩擦–黏性土边坡安全系数为[25]:

$$F_S = \min\left(\frac{c'}{\gamma z}\cdot\frac{1}{\left((1+k_v)\sin\beta\cos\beta + k_h\cos^2\beta\right)} + \frac{(1+k_v)\cos\beta - k_h\sin\beta}{(1+k_v)\sin\beta + k_h\cos\beta}\tan\phi'\right) \tag{7}$$

式中,$0 < z \le H$,c'为有效黏聚力。

由式(7)可知:当参数c'、ϕ'、γ、β、k_h、k_v保持不变时,最小值出现在无限长边坡最底部。因此,地震作用下无限长摩擦–黏性土边坡安全系数为:

$$F_S = \frac{c'}{\left((1+k_v)\sin\beta\cos\beta + k_h\cos^2\beta\right)\gamma H} + \frac{\left((1+k_v)\cos^2\beta - k_h\sin\beta\cos\beta\right)\gamma H\tan\phi'}{\left((1+k_v)\sin\beta\cos\beta + k_h\cos^2\beta\right)\gamma H} \tag{8}$$

地震作用下无限长摩擦–黏性土边坡安全系数的表达式中参数较多,现将式(8)适当转化,两边同时除以$\tan\phi'$可得:

$$\frac{F_S}{\tan\phi'} = \frac{c'}{\gamma H\tan\phi'}\cdot\frac{1}{((1+k_v)\sin\beta\cos\beta + k_h\cos^2\beta)} + \frac{(1+k_v)\cos\beta - k_h\sin\beta}{(1+k_v)\sin\beta + k_h\cos\beta} \tag{9}$$

本文采用无量纲参数$S = c'/(\gamma H\tan\phi')$[27],将式(9)进一步表示为:

$$\frac{F_S}{\tan\phi'} = \frac{S}{(1+k_v)\sin\beta\cos\beta + k_h\cos^2\beta} + \frac{(1+k_v)\cos\beta - k_h\sin\beta}{(1+k_v)\sin\beta + k_h\cos\beta} \tag{10}$$

水平地震力系数k_h=0.1、0.2、0.3时,不同λ和S条件下$F_S/\tan\phi'$与β的关系曲线分别如图8~10所示。由图8~10可知:随着β的增大,$F_S/\tan\phi'$先减小后增大,说明地震力作用下无限长摩擦–黏性土边坡存在一个最危险坡度$\beta_{\min}$;当k_h和λ一定时,$F_S/\tan\phi'$随着S的增大而增大,$\beta_{\min}$随着S的增大而减小;当k_h较小时(k_h=0.1),竖向地震力对边坡稳定性的影响并不大,随着k_h的增大,竖向地震力对边坡稳定性的影响逐渐显著;此外,同一方向的竖向地震力作用对于无限长摩擦–黏性土边坡稳定性的影响并不是单一地有利于稳定或不利于稳定,还与k_h、β、S有关。以图10(c)为例:当β为10°时,$F_S/\tan\phi'$随着λ的增大而增大;当β为80°时,$F_S/\tan\phi'$随着λ的增大而减小。这是因为无限长边坡安全系数为潜在破坏面上抗滑力与滑动力的比值,而k_h、β、S的变化均会影响潜在破坏面上抗滑力与滑动力的比值。

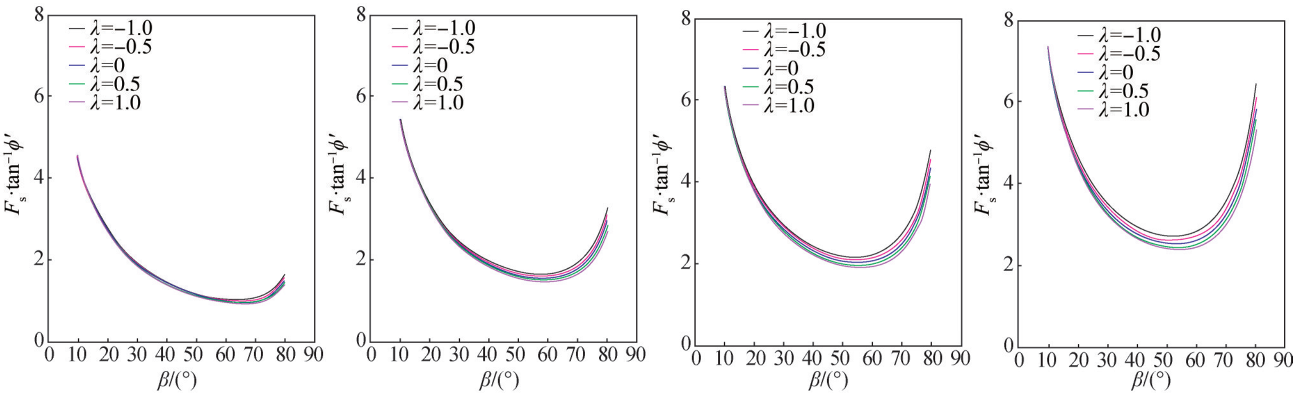

(a) S=0.25 (b) S=0.50 (c) S=0.75 (d) S=1.00

图8 $k_h=0.1$时不同λ和S条件下$F_S/\tan\phi'$与β的关系

Fig. 8 Relationship of $F_S/\tan\phi'$ with β for different λ and S when $k_h=0.1$

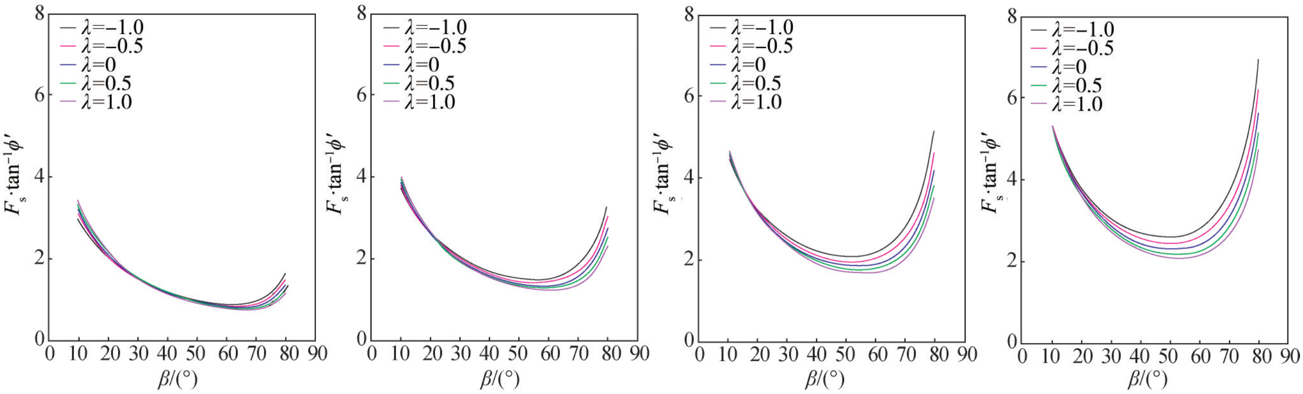

(a) S=0.25 (b) S=0.50 (c) S=0.75 (d) S=1.00

图9 $k_h=0.2$时不同λ和S条件下$F_S/\tan\phi'$与β的关系

Fig. 9 Relationship of $F_S/\tan\phi'$ with β for different λ and S when $k_h=0.2$

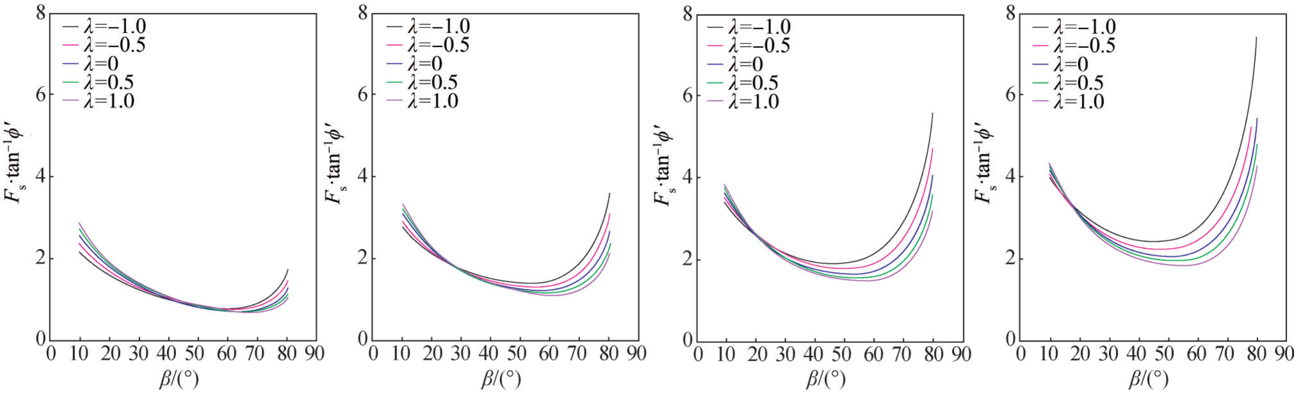

(a) S=0.25 (b) S=0.50 (c) S=0.75 (d) S=1.00

图10 $k_h=0.3$时不同λ和S条件下$F_S/\tan\phi'$与β的关系

Fig. 10 Relationship of $F_S/\tan\phi'$ with β for different λ and S when $k_h=0.3$

由于地震作用下无限长摩擦–黏性土边坡$F_S/\tan\phi'$的表达式较为复杂，难以直接求$\beta_{\min}$的解析式。根据最危险坡度的定义，在不同条件下将不同β分别代入$F_S/\tan\phi'$的表达式中进行计算，通过记录（每隔0.01°记录一个数值）使无限长摩擦–黏性土边坡取得最小$F_S/\tan\phi'$的β，获得对应条件下的$\beta_{\min}$。图11为k_h取0.1、0.2和0.3时，不同λ和S条件下无限长摩擦–黏性土边坡最危险坡度$\beta_{\min}$。由图11可知：当k_h和S一定时，$\beta_{\min}$随λ的增大而增大。当S一定时，随着λ从−1.0增大至1.0，k_h=0.1对应$\beta_{\min}$增大约2.0°，k_h=0.2对应

$\beta_{\min}$增大约4.5°，k_h=0.3对应$\beta_{\min}$增大约7.3°，说明随着k_h的增大，竖向地震力作用对无限长摩擦–黏性土边坡$\beta_{\min}$的影响逐渐显著。

图12为k_h=0.1、0.2和0.3时，不同λ条件下无限长摩擦–黏性土边坡最危险坡度$\beta_{\min}$与无量纲参数S的关系曲线。由图12可知：最危险坡度$\beta_{\min}$随着S的增大而逐渐减小，直至趋于一个稳定值；当S相同时，最危险坡度$\beta_{\min}$随着λ的增大而增大；随着水平地震力系数k_h的增大，竖向地震力作用对最危险坡度$\beta_{\min}$的影响逐渐显著，特别是在S的值较大的情况下。

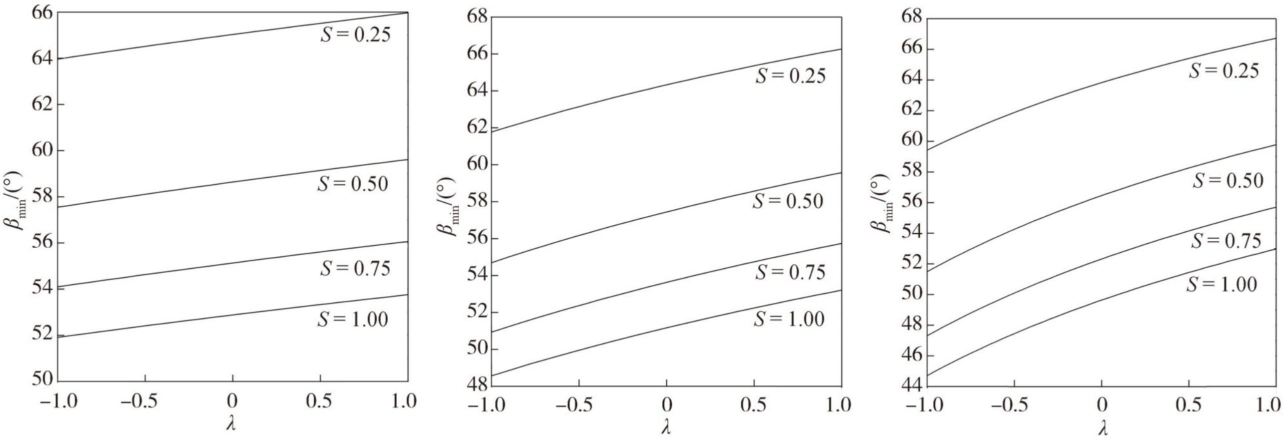

(a) k_h=0.1　(b) k_h=0.2　(c) k_h=0.3

图11　不同λ和S条件下边坡最危险坡度$\beta_{\min}$

Fig. 11　Critical slope angles for slopes with different λ and S

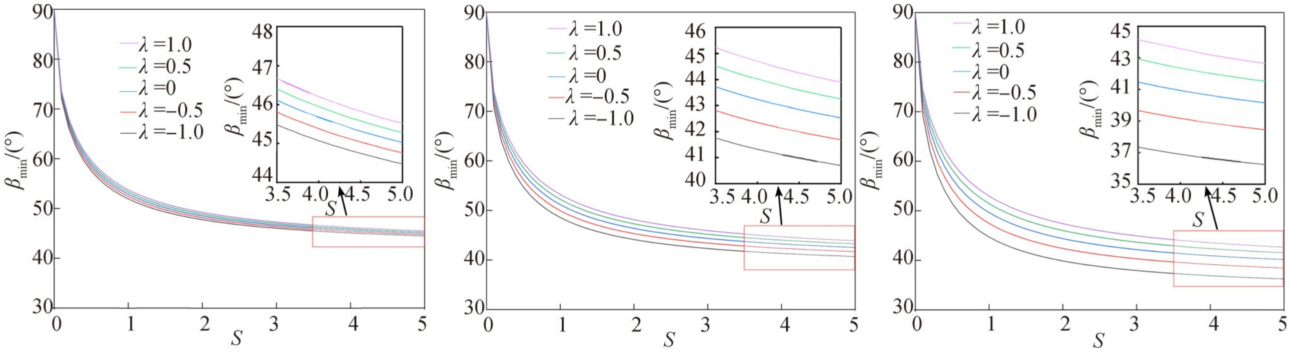

(a) k_h=0.1　(b) k_h=0.2　(c) k_h=0.3

图12　不同λ条件下边坡最危险坡度$\beta_{\min}$与S的关系

Fig. 12　Critical slope angle versus the S for different λ

2.2　可靠度分析

为研究地震力作用对无限长摩擦–黏性土边坡可靠度的影响，算例边坡取值如下：$H=5$ m，$\gamma=17$ kN/m^3，有效黏聚力均值$\mu_{c'}=10$ kPa，有效黏聚力变异系数$v_{c'}=0.3$，均值$\mu_{\tan\phi'}=0.5774$，变异系数$v_{\tan\phi'}=0.3$，相关系数$\rho_{c'\tan\phi'}=0$，$\beta=30°$。本文不考虑c'和ϕ'之间的相关性（即相关系数$\rho_{c'\tan\phi'}=0$）。图13为当$k_h=0.1$和0.2时，不同λ条件下无限长摩擦–黏性土边坡失效概率p_f与无量纲相关距离Θ的关系曲线。由图13(a)可以看出：当k_h=0.1时，p_f随着Θ的增大而减小；在相同的Θ下，当λ从−1.0增大至1.0时，p_f增大，即此时竖直向下的地震力增大了边坡失效概率。由图13(b)可知，在相同的Θ下，当λ从−1.0增大至1.0时，p_f降低，此时竖直向下的地震力减小了边坡失效概率。该结论与确定性分析结果一致，即同一方向的竖向地震力作用对于无限长摩擦–黏性土边坡稳定性的影响并不是单一地有利于边坡稳定或不利于边坡稳定，还与k_h、β、S有关。

图14为算例边坡在$\mu_{c'}=49.08$ kPa，$\Theta=4$，$k_h=0.2$，$k_v=-0.1$时失效概率与边坡坡度的关系曲线。此时，无量纲参数S的均值$\mu_S=49.08/(17\times5\times0.5774)\approx1.0$。由图14可知，当$k_h$=0.2、$k_v=-0.1$、$\beta=50°$时，边坡失效概率最大，这与确定性分析图11(b)中的最危险坡度值对应。

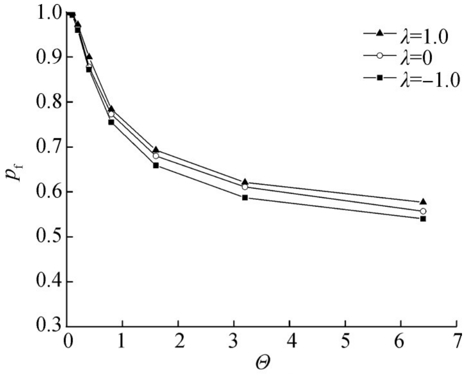

(a) k_h=0.1

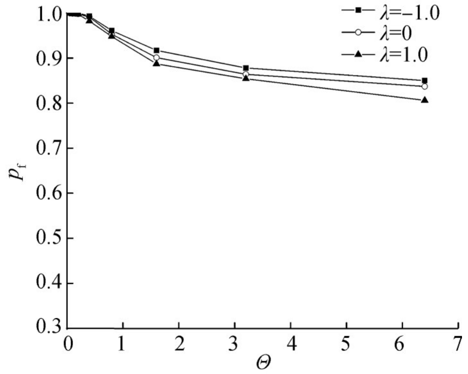

(b) k_h=0.2

图13 不同λ条件下失效概率与无量纲相关距离关系

Fig. 13 Relationship of p_f with Θ for different λ

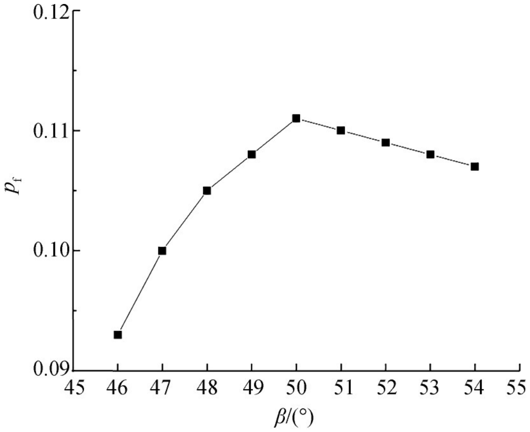

图14 地震边坡失效概率与边坡坡度关系

Fig. 14 p_f versus β for an infinite seismic slope

3 结 论

本文采用随机场方法对地震作用下无限长边坡进行了可靠度分析，并基于确定性分析方法进行了验证。主要结论如下：

1）对于地震作用下的无限长边坡，即使k_h较小，竖向地震力对无限长边坡的失效概率p_f仍有明显影响，因此对地震作用下无限长边坡进行可靠度分析时，水平和竖向地震力作用均不可忽略。

2）对于无限长不排水边坡，存在一个β_{min}使边坡失效概率最大。k_h一定时，β_{min}随着λ的增大而增大。随着k_h增大，竖向地震力作用对β_{min}的影响逐渐增强。

3）对于无限长摩擦–黏性土边坡，同样存在一个β_{min}使得p_f最大。β_{min}随着无量纲参数S的增大而逐渐减小，直至趋于一稳定数值；当S相同时，最危险坡度随着λ的增大而增大。随着水平地震力系数的增大，竖向地震力作用对最危险坡度的影响逐渐显著；随着S值的增大，该影响更为显著。

参考文献：

[1] Ji Jian,Gao Yufeng,Lü Qing,et al.China's early warning system progress[J].Science,2019,365(6451):332.

[2] Sahoo P P,Shukla S K.Taylor's slope stability chart for combined effects of horizontal and vertical seismic coefficients[J].Géotechnique,2019,69(4):344–354.

[3] Cui Hongzhi,Ji Jian,Song Jian,et al.Limit state line-based seismic stability charts for homogeneous earth slopes[J]. Computers and Geotechnics,2022,146:104749.

[4] Huang Wengui,Ji Jian.Closed-form solutions for regional earthquake-induced landslide prediction:Rotational failure mechanism[J].Landslides,2022,19(11):2671–2684.

[5] Sinchith M,Nandi S,Ghosh P.Critical stability analysis of slopes using stress characteristics in purely cohesive soil [J]. International Journal of Geomechanics, 2023, 23(1): 04022263.

[6] Song Jian,Wu Kaili,Feng Tugen,et al.Coupled analysis of earthquake-induced permanent deformations at shallow and deep failure planes of slopes[J].Engineering Geology,2020, 274:105688.

[7] Song Jian,Rodriguez–Marek A,Feng Tugen,et al.A generalized seismic sliding model of slopes with multiple slip surfaces[J].Earthquake Engineering & Structural Dynamics,2021,50(10):2595–2612.

[8] Cheng Yin,Wang Jianfeng,He Yi.Prediction models of newmark sliding displacement of slopes using deep neural network and mixed-effect regression[J]. Computers and Geotechnics,2023,156:105264.

[9] Wang Maoxin,Wu Qiang.Artificial neural network-aided decoupled prediction of earthquake-induced shallow and deep sliding displacements of slopes[J].Computers and Geotechnics,2023,164:105844.

[10] Ma Zongyuan, Liao Hongjian, Dang Faning, et al. Seismic slope stability and failure process analysis using explicit finite element method[J]. Bulletin of Engineering Geology and the Environment,2021,80(2):1287–1301.

[11] Li Cheng,Su Lijun,Liao Hongjian,et al.Modeling of rapid evaluation for seismic stability of soil slope by finite elem-

ent limit analysis[J].Computers and Geotechnics,2021,133:104074.

[12] Hwang Y W,Rathje E M.Insights into seismic slope deformation patterns using finite element analysis[J].Soil Dynamics and Earthquake Engineering,2023,164:107660.

[13] Qin Changbing,Zhou Jianfeng.On the seismic stability of soil slopes containing dual weak layers:True failure load assessment by finite-element limit-analysis[J].Acta Geotechnica,2023,18(6):3153–3175.

[14] Phoon K K,Kulhawy F H.Characterization of geotechnical variability[J].Canadian Geotechnical Journal,1999,36(4):612–624.

[15] Shu Shuang,Ge Bin,Wu Yongxin,et al.Probabilistic assessment on 3D stability and failure mechanism of undrained slopes based on the kinematic approach of limit analysis[J]. International Journal of Geomechanics, 2023, 23(1): 06022037.

[16] He Yi,Li Zhi,Ou Jialong,et al.Random finite-element analysis of slope considering strength anisotropy and spatial variability of soil[J].Natural Hazards Review,2024,25(2):04024010.

[17] Jin Baoming,Lin Peng,Lee Kwantun.Integrating kinematic subsurface-wave approximation with infinite-slope stability analysis for landslide predictions[J].Advanced Engineering Sciences,2021,53(4):140–148.[金保明,林鹏,李光敦.基于运动波壤中流理论与无限边坡稳定分析理论的滑坡预测模型[J].工程科学与技术,2021,53(4):140–148.]

[18] 赵炼恒,李亮,杨峰,等.边坡稳定性非线性能耗分析理论[M].北京:科学出版社,2019.

[19] Griffiths D V,Huang Jinsong,Fenton G A.Probabilistic infinite slope analysis[J].Computers and Geotechnics,2011,38(4):577–584.

[20] Cai Jingsen,Yan Echuan,Yeh T J,et al.Effect of spatial variability of shear strength on reliability of infinite slopes using analytical approach[J]. Computers and Geotechnics, 2017,81:77–86.

[21] Zhu Bin,Pei Huafu,Yang Qing.Reliability analysis of submarine slope considering the spatial variability of the sediment strength using random fields[J].Applied Ocean Research,2019,86:340–350.

[22] Zhu D,Griffiths D V,Huang J,et al.Probabilistic stability analyses of undrained slopes with linearly increasing mean strength[J].Géotechnique,2017,67(8):733–746.

[23] Zhu Desheng,Xia Lei,Griffiths D V,et al.Reliability analysis of infinite slopes with linearly increasing mean undrained strength[J].Computers and Geotechnics,2021,140:104442.

[24] 胡聿贤.地震工程学[M].北京:地震出版社,2006.

[25] Yang J.On seismic landslide hazard assessment[J].Géotechnique,2007,57(8):707–713.

[26] Fenton G A,Vanmarcke E H.Simulation of random fields *via* local average subdivision[J].Journal of Engineering Mechanics,1990,116(8):1733–1749.

[27] Bell J M.Dimensionless parameters for homogeneous earth slopes[J].Journal of the Soil Mechanics and Foundations Division,1966,92(5):51–65.

Reliability Analysis of Infinite Slopes Subjected to Seismic Loadings Considering Spatially Variable Shear Strength Parameters

ZHU Desheng[1], *XIA Lei*[2], *KE Lijun*[1], *WANG Zhen*[1*]

(1.College of Civil Science and Engineering, Yangzhou University, Yangzhou 225127, China;
2.School of Civil Engineering, Southeast University, Nanjing 211189, China)

Abstract:

Objective Evaluating seismic slope stability is a critical research topic in the field of geotechnical engineering. Natural soils exhibit spatial variability, with properties varying from point to point. This characteristic significantly affects slope stability, necessitating a statistical approach to its investigation. The infinite slope model evaluates the stability of long slopes running down a hillside and analyzes the mechanics of shallow landslides. This study focuses on the reliability of infinite undrained slopes and cohesive-frictional soil slopes subjected to seismic loadings using the random field method.

Methods The random field method was adopted to investigate the effects of horizontal and vertical seismic loadings on the reliability of infinite slopes. The deterministic method was also employed to verify the results obtained by the random field method. For deterministic stability analyses of infinite undrained slopes with linearly increasing strength, the infinite slope equation was utilized to evaluate the factor of safety F_S and derive the analytical formula for the critical slope angle $\beta_{\min}$, which leads to the minimum factor of safety F_S. An algorithm generating 1D non-stationary random fields of undrained strength was applied to assess the probability of slope failure pf and determine the critical slope angle $\beta_{\min}$, which corresponds to the maximum probability of slope failure p_f. For deterministic analyses of infinite cohesive-frictional soil slope stability, the infinite slope equation was employed to analyze the factor of safety F_S, with the critical slope angle min obtained by calculating the factor of safety F_S at intervals of 0.01. The random field method was then applied to compute the probability of slope failure p_f and determine the critical slope angle $\beta_{\min}$.

Results and Discussions For the infinite undrained slopes subjected to horizontal and vertical seismic loadings, the results showed that as the slope angle β increases, the factor of safety F_{S} initially decreases and then increases, indicating the existence of a critical slope angle $\beta_{\min}$. As the value of λ (ratio of the vertical seismic coefficient kv to the horizontal seismic coefficient k_{h}) increases, the critical slope angle min gradually rises, and the effect of the vertical seismic loading on the critical slope angle $\beta_{\min}$ becomes more significant as the horizontal seismic coefficient k_{h} increases. The results also indicated that as the value of λ increases, the probability of slope failure pf increases significantly, highlighting that the effect of the vertical seismic loading on the reliability of infinite undrained slopes cannot be ignored.In addition, the probability of slope failure p_{f} decreases as the nondimensional spatial correlation length Θ increases and eventually converges asymptotically on the first-order second moment (FOSM) solution, demonstrating that the traditional reliability method may provide unconservative results for infinite undrained slopes subjected to seismic loadings. The analysis further reveals the existence of a critical slope angle $\beta_{\min}$, which leads to the maximum value of the probability of slope failure p_{f}, a phenomenon that can also be verified by the deterministic method. For the infinite cohesive-frictional soil slopes subjected to horizontal and vertical seismic loadings, the results showed that as the slope angle β increases, the value of $F_{\mathrm{S}}/\tan\phi'$ initially decreases and then increases, indicating the existence of a critical slope angle min. The value of $F_{\mathrm{S}}/\tan\phi'$ increases as the nondimensional parameter $S = c/(H\tan\phi')$ increases, while the critical slope angle $\beta_{\min}$ decreases as the nondimensional parameter S increases. When the horizontal seismic coefficient k_{h} is relatively small, the effect of the vertical seismic loading on the stability of infinite cohesive-frictional soil slopes is not significant. However, as the horizontal seismic coefficient k_{h} increases, the effect of the vertical seismic loading becomes more pronounced. In addition, the influence of the vertical seismic loading on the stability of infinite cohesive-frictional soil slopes is affected by the horizontal seismic coefficient k_{h}, the slope angle β, and the nondimensional parameter S. The critical slope angle $\beta_{\min}$ increases as the value of λ increases, and the effect of the vertical seismic loading on the critical slope angle $\beta_{\min}$ for infinite cohesive-frictional soil slopes becomes more evident as the horizontal seismic coefficient k_{h} increases. The critical slope angle $\beta_{\min}$ decreases as the nondimensional parameter S increases and eventually stabilizes. The critical slope angle $\beta_{\min}$ increases as the value of λ rises. As the horizontal seismic coefficient k_{h} improves, the effect of the vertical seismic loading on the critical slope angle $\beta_{\min}$ becomes increasingly significant, particularly for higher values of the nondimensional parameter S. Some results indicate that the probability of slope failure p_{f} increases as the value of λ increases. In contrast, others show a decrease in the probability of slope failure p_{f} as the value of λ increases. This phenomenon can also be confirmed by the deterministic method. There exists a critical slope angle $\beta_{\min}$ that leads to the maximum probability of slope failure p_{f}, with the critical slope angle $\beta_{\min}$ being consistent with previous results.

Conclusions For infinite slopes subjected to seismic loadings, the effect of the vertical seismic loading on the probability of slope failure pf remains significant even when the horizontal seismic coefficient k_{h} is small. Both horizontal and vertical seismic loadings must be considered when performing seismic reliability analyses of infinite slopes. There exists a critical slope angle $\beta_{\min}$ that results in the maximum probability of slope failure p_{f} for infinite slopes. In addition, the influence of the vertical seismic loading on the critical slope angle $\beta_{\min}$ becomes increasingly apparent as the horizontal seismic coefficient k_{h} increases.

Key words: infinite slope; seismic loading; critical slope angle; reliability analysis; random field simulation

（编辑　周　璇）

引用格式: Zhu Desheng,Xia Lei,Ke Lijun,et al.Reliability analysis of infinite slopes subjected to seismic loadings considering spatially variable shear strength parameters[J].Advanced Engineering Sciences,2025,57(3):106–114.[朱德胜,夏磊,柯力俊,等.考虑土体参数空间变异性的地震作用下无限长边坡可靠度研究[J].工程科学与技术,2025,57(3):106–114.]